Magnetostructural Coupling in Magnetocaloric MnSb via X-ray and Neutron Scattering

Blake Hawkins

A senior thesis submitted to the faculty of
Brigham Young University
in partial fulfillment of the requirements for the degree of

Bachelor of Science

Dr. Benjamin Frandsen, Advisor

Department of Physics and Astronomy

Brigham Young University

ABSTRACT

Magnetostructural Coupling in Magnetocaloric MnSb via X-ray and Neutron Scattering

Blake Hawkins
Department of Physics and Astronomy, BYU
Bachelor of Science

Magnetocaloric materials have drawn significant research interest for their potential in environmentally friendly solid-state refrigeration and waste-heat recovery technologies. Manganese antimony (MnSb) is a promising candidate due to its high refrigerant capacity and tunable magnetic properties. As with many magnetocaloric materials, magnetostructural coupling plays a key role in its performance. Here, we investigate the magnetostructural behavior of stoichiometric MnSb, which undergoes a transition to a ferromagnetic state at its Curie temperature ($T_C = 577$ K). Our analysis uses temperature-dependent x-ray and neutron diffraction, along with pair distribution function analysis. The results reveal strong magnetoelastic coupling, with a volume expansion of over 0.5% upon cooling into the ferromagnetic state, relative to the non-magnetic trend. Spontaneous magnetostriction of this magnitude is very rare. Notably, the lattice response begins above T_C, driven by the growth of short-range ferromagnetic correlations. Additionally, field-dependent measurements confirm the presence of field-induced magnetostriction with a nontrivial temperature dependence. These findings provide new insight into the magnetostructural behavior of MnSb, furthering its potential as a powerful magnetocaloric material.

Keywords: Magnetocalorics, MCE, Magnetostriction, MnSb, Refrigeration, Waste Heat, Solid State, PDF, mPDF, NSLS II, Magnetostructural Coupling

ACKNOWLEDGMENTS

I would like to acknowledge the US Department of Energy, Office of Science, Basic Energy Sciences for funding this research. This research used beamline 28-ID-1 of the National Synchrotron Light Source II, a U.S. Department of Energy (DOE) Office of Science User Facility operated for the DOE Office of Science by Brookhaven National Laboratory under Contract no.DE-SC0012704. I would like to thank Raju Baral for his preliminary research on MnTe and his role in synthesizing our MnSb sample. I also want to thank Dr. Benjamin Frandsen for his support and expertise on this topic–I could not have done this without him.

List of Figures

1 Introduction

A major goal of condensed matter physics is to understand and utilize the properties of materials for the betterment of life on earth. Our research focuses on the potential magnetocaloric properties of a specific material, MnSb. These properties have the potential to improve the efficiency and reduce environmental impact of current methods of refrigeration and waste heat recovery. Our research is focused on probing the atomic and magnetic structure of MnSb to better understand the properties that make it a promising magnetocaloric candidate.

1.1 Magnetocalorics

The Magnetocaloric Effect (MCE) occurs when an applied magnetic field causes a reversible temperature change in a material [1]. The external magnetic field aligns the magnetic spins in a magnetocaloric material. The sudden alignment of spins reduces the intrinsic entropy of the system. In order to satisfy the second law of thermodynamics, the temperature of the material will then increase and release heat. If cycled correctly, this effect can be harnessed in refrigeration. The reverse magnetocaloric effect (RMCE), on the other hand, occurs when a change in external temperature induces a change in the magnetic field. This change in magnetic field can be harnessed to produce mechanical energy and electricity from waste heat. These environmental applications are especially pertinent now, given the global need to mitigate and adapt to a rapidly changing climate.

1.2 Manganese Antimony (MnSb)

The ferromagnetic metal, manganese antimony (MnSb), has recently attracted significant interest as a potential high-performance magnetocaloric material [2]. In a ferromagnet the magnetic spins are aligned parallel to each other, even without an external magnetic field. MnSb transitions from a ferromagnet to a paramagnet at temperatures above 577 K. This transition temperature is termed the Curie temperature. Above the Curie temperature, thermal energy disrupts the alignment of the magnetic domains, causing the material to lose its spontaneous magnetization and become a paramagnet. MnSb's particularly promising properties are due in large part to short-range magnetic correlations in the paramagnetic state.

The magnitude of the MCE is correlated with the change in volume of the physical unit cell in response to an applied magnetic field. This phenomenon is called forced magnetostriction. The change in the size of the unit cell across the transition temperature in the absence of an applied field is known as spontaneous magnetostriction. magnetostriction.

By studying this unique material, we identified MnSb as a strong candidate in the search for useful magnetocaloric materials. A useful candidate would have a strong MCE and a tunable transition temperature–both of which are manifest in MnSb [3]. Understanding the magnetocaloric properties of MnSb may be crucial for developing efficient, environmentally friendly refrigeration and energy conversion technologies. By studying MnSb's magnetic transitions and structural changes, we can optimize materials for sustainable cooling and waste heat recovery.

The question is, how does the structure and magnetism of Manganese Antimony change across the Curie temperature and in an applied magnetic field? My research and this paper attempt to fully address this question. First we will address the methodology of our research, then transition into the results. Finally, I will draw conclusions and contextualize our findings within the broader scope of past and future studies.

2 Methods

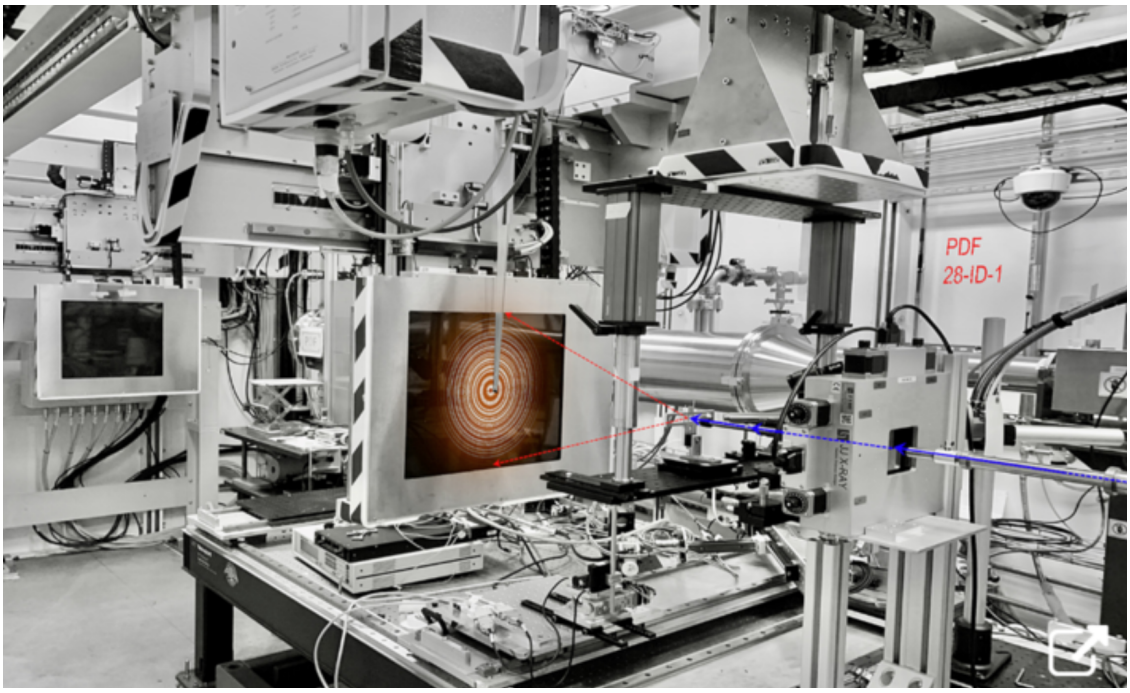

Figure 2.1 NSLS II, Beamline 28, at Brookhaven National Laboratory. Here the blue line indicates a concentrated beam of x-rays. These x-rays hit the sample and diffract onto the sensor as indicated by the red arrows.

2.1 Synchrotron X-ray Diffraction Experiments

We conducted our experiments at Brookhaven National Laboratory (BNL) using the National Synchrotron Light Source II (NSLS-II) [4]. A synchrotron first accelerates high-energy electrons

to produce photons in the x-ray range of the electromagnetic spectrum. The machine concentrates the x-rays onto our material. The x-rays scatter off of our fine powder sample creating a pattern of concentric rings on the sensor. We are able to perform a Fourier transform on the pattern, which yields a pair distribution function (PDF). From the PDF, we can extract data about the proximity of the atoms and the size of the unit cell. The primary goal of our first experiment was to investigate the effect of a varied applied magnetic field on the lattice parameters of the unit cell at different temperatures. Our second experiment focused on the spontaneous magnetostriction that occurred across T_C in zero applied field.

2.1.1 Magnetic Field Dependence at Fixed Temperatures

First we examined the effect of an external magnetic field on the lattice structure at different fixed temperatures. Using PDF analysis of the x-ray diffraction (XRD) data we compared the evolution of the *a* and *c* lattice parameters to the changing applied magnetic field. For each temperature, we gradually increased the applied field from 0 to 5 T while recording diffraction data. This process was repeated at temperatures of 10 K, 100 K, 200 K, 300 K, 400 K, and 500 K.

2.1.2 Temperature-Dependent Measurements Across the T_C

In the second phase of the experiment, we returned to NSLS-II to investigate the structural evolution across the Curie temperature (577 K). This time, measurements were taken in zero field while continuously heating the sample using a hot air blower. XRD data were collected as we increased the temperature past the T_C and subsequently as the sample was cooled back down. Again we used PDF analysis to extract the *a* and *c* lattice parameters this time as a function temperature.

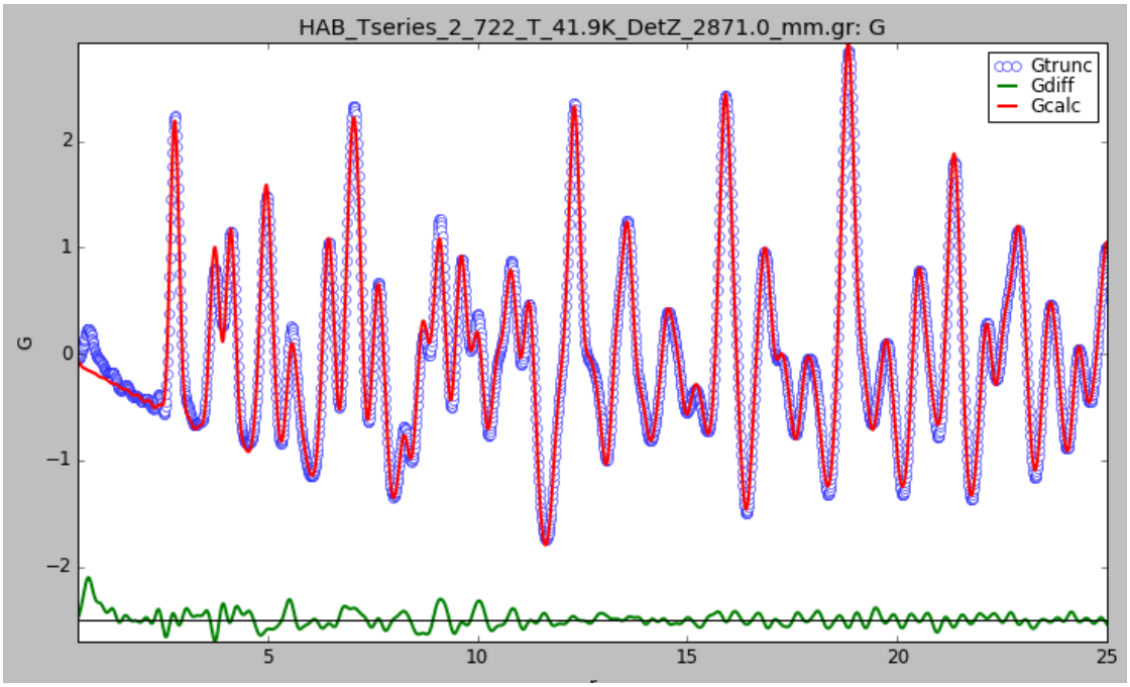

Figure 2.2 X-ray Pair Distribution Function. The x axis is in units of Angstroms. The y axis is the related to the probability density. The Pair Distribution Function provides information about the lattice structure. Peaks in the function correspond to preferred atomic distance. In other words, a peak represents a distance where atoms are more likely to be found relative to one another.

2.2 Neutron Diffraction Experiment

A complementary experiment was performed using neutron scattering data, in order to obtain the magnetic pair distribution function data (mPDF). Using neutron diffraction allows one to extract the magnetic component of the PDF and analyze both local and average magnetic order parameters. [5]

The neutron scattering data allowed for a direct comparison between x-ray scattering results obtained at NSLS-II and the neutron scattering data. The structural trends observed in both techniques were analyzed to ensure consistency and better understand the underlying mechanisms governing the lattice parameter evolution [3]. These comparisons and results can be seen below.

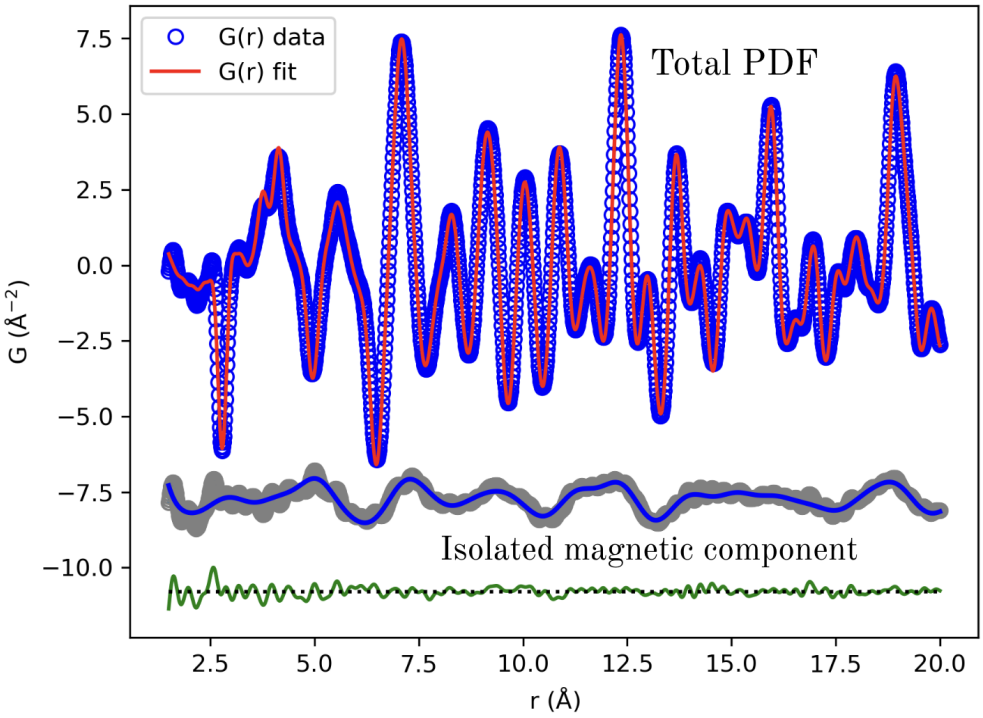

Figure 2.3 Neutron PDF with separated mPDF data. Here we can see the Neutron PDF data which contains the same structural information as the x-ray PDF, but also includes information about the magnetic correlations between neighboring spins. The separated magnetic signal can be seen in gray below the atomic PDF data.

3 Results

The results presented below demonstrate strong magnetostructural coupling in MnSb, including forced magnetostriction in an applied field and spontaneous magnetostriction in zero field. I will first present the zero-field results, then the results with an applied field, and finally the magnetic PDF results.

3.1 Magnetostructural Coupling in Zero Applied Field

First, we performed fits of the hexagonal structural model of MnSb to the x-ray and neutron PDF data collected at various temperatures above and below the Curie temperature. From these fits, the a and c lattice parameters were extracted as a function of temperature, as plotted in Fig. 3.1. To analyze the temperature-dependent structural changes, we fit a linear model to the high-temperature region (above the Curie transition). This provided a baseline for evaluating the fractional deviation of the measured lattice parameters from the expected high-temperature trend. The deviation from the linear, high-temperature, volumetric expansion of the unit cell can largely be attributed to the Pauli Exclusion Principle. The Pauli Exclusion Principle states that no two fermions in can occupy the same quantum state at the same time. At high temperatures, in the paramagnetic state, the magnetic spins in our sample were unaligned, so Pauli's Principle did not apply. However, as the material cools into the ferromagnetic state, the spins begin to realign. In accordance with the Pauli Exclusion Principle, the unit cell expands in order avoid overlapping spins. This was demonstrated

in our x-ray and neutron scattering data. This is the reverse of what happens in antiferromagnetic materials when they go through a magnetic transition [2]. Both the x-ray and neutron scattering data compared to the slope lines over a wide temperature range are shown in Fig. 3.2. The high temperature slopes and fractional volume differences for both the x-ray and neutron data are very comparable.

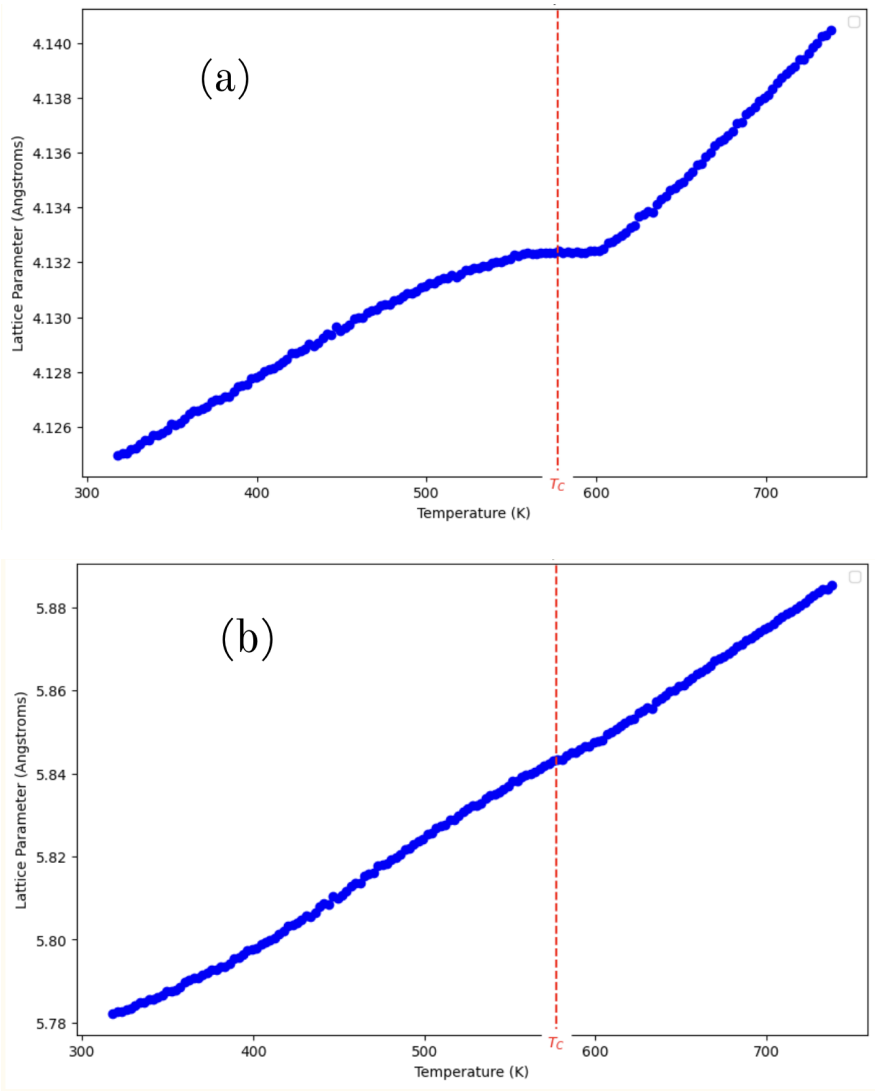

Figure 3.1 Anisotropic responses from a lattice (a) and c lattice (b) parameters across transition temperature. The transition temperature or Curie Temperature is marked by the red dashed line. Note in both cases there is a clear deviation from the linear trend well before the transition temperature as discussed further in the main text.

The volume expansion before the transition temperature means that short range magnetic order is driving a physical response well before long range order comes into effect. The data clearly show that the a and c lattice parameters expand differently across the transition temperature. Thus, the interactions within the crystal are described as anisotropic . If the unit cell were cubic, we would

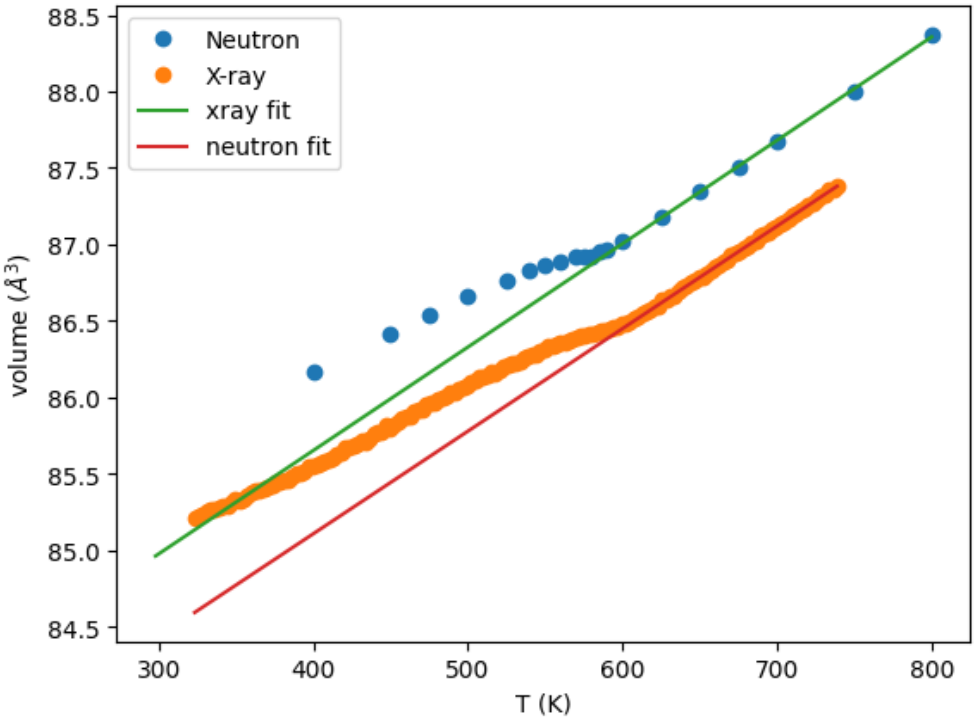

Figure 3.2 Comparison of x-ray and neutron PDF data factoring out linear temperature dependent expansion. There is a slight offset in the measured volume from neutron and x-ray diffraction. We can safely attribute this to calibration differences. Note the clear deviation from the slope line right above the Curie Temperature of 577 K.

expect the lattice parameters to have an isotropic reaction to the magnetic transition. But MnSb has a NiAs hexagonal crystal structure type. Bonds in the plane are different from bonds above and below the plane. Elastic energy of bonds and magnetic exchange interactions have different strengths in plane and out of plane.

3.2 Structural Response in an Applied Magnetic Field

Unexpectedly, observed the strength of the magnetostrictive response varied at different temperatures. At different temperatures the effect of the applied magnetic field on the size of the unit cell was different. This can be seen very clearly in Fig. 3.3, where the a lattice expands with increasing field at 10 K, but shows no systematic behavior at 400 K. This indicates nontrivial temperature dependence of the sign and magnitude of the magnetostriction coefficient in MnSb.

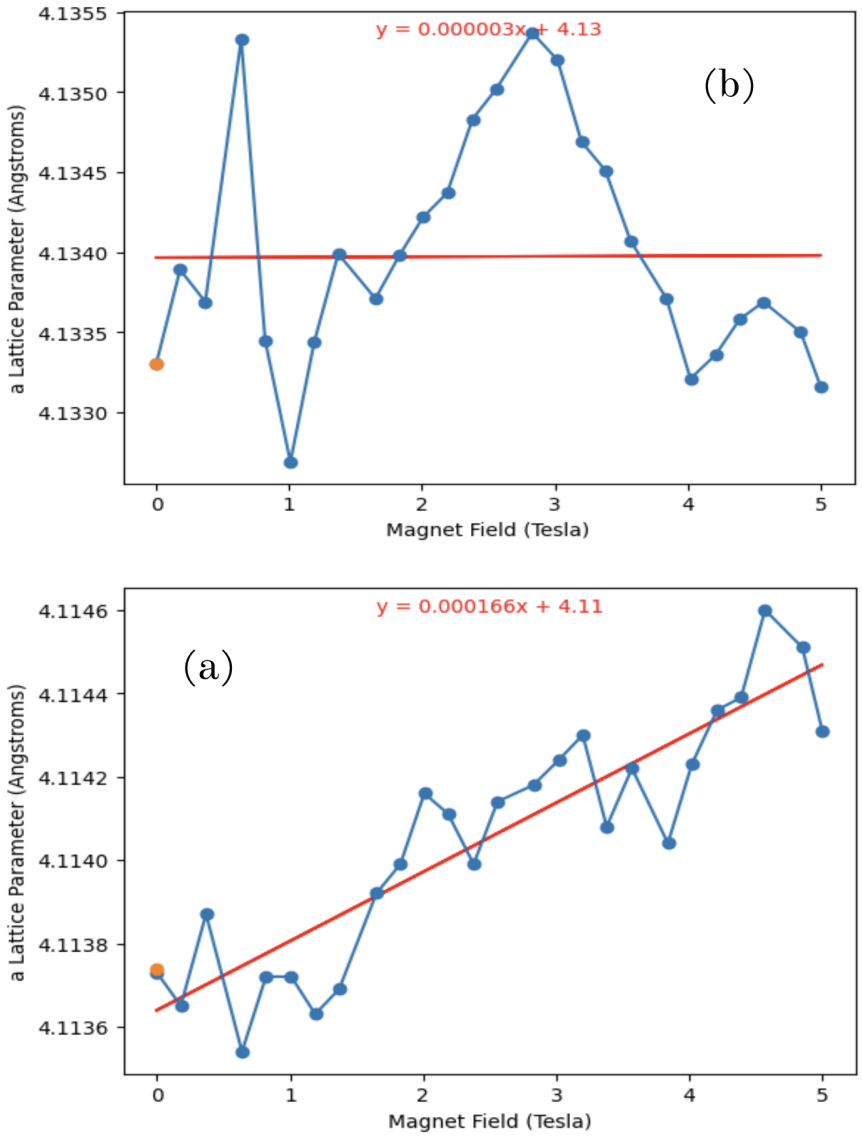

Figure 3.3 Measured c lattice parameters as a function of applied magnetic field. At certain temperatures, like 10 K (a), there was a clear positive relationship between the applied field and the lattice parameters. While at other temperatures, like 400 K (b), the field and lattice parameters shows no relationship at all.

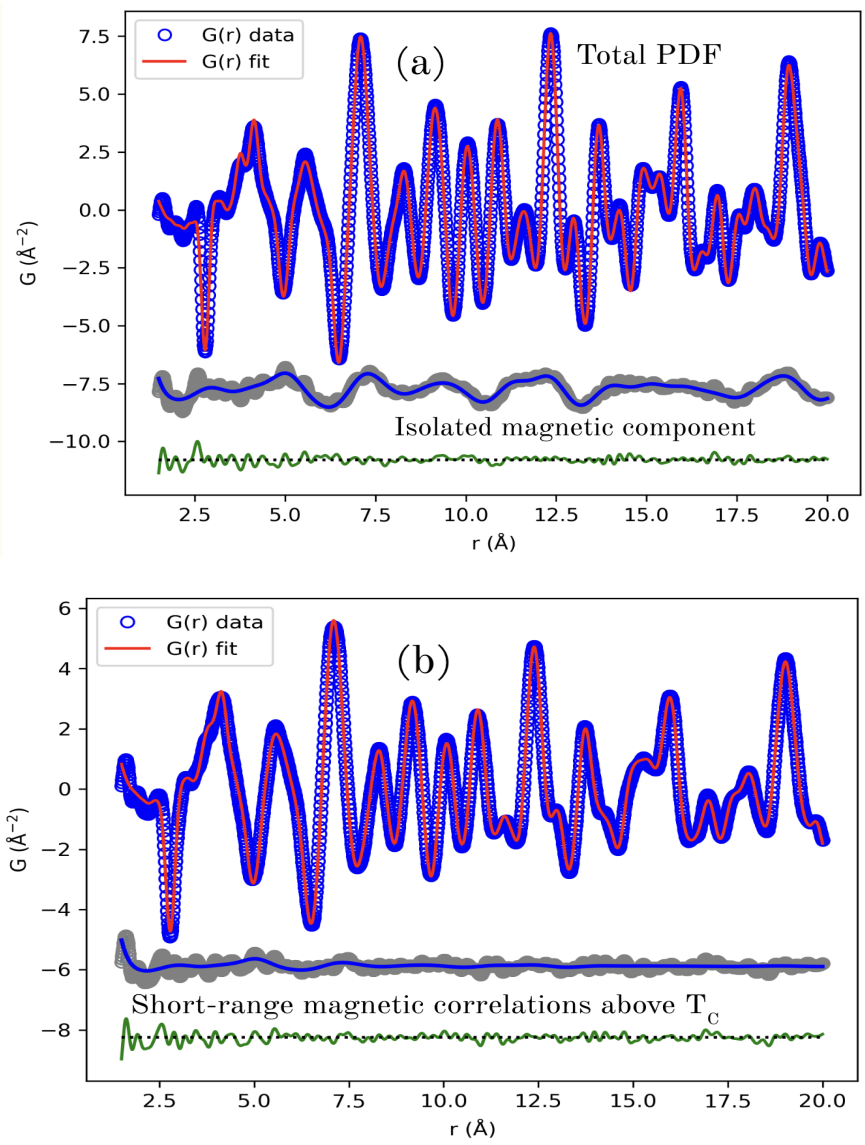

Figure 3.4 Neutron PDF data above and below T_C. Note that below T_C there is a clear long range magnetic signal. While above the transition temperature, the long range signal dies off. We can still extract the local magnetic order parameter by fitting the magnetic signal over a much smaller range

3.3 Magnetic Parameters

Representative neutron PDF fits, including the magnetic PDF component, are shown in Fig. 3.4.

The isolated magnetic PDF component confirms the sensitivity of the data to the local magnetic

correlations in MnSb. By fitting the mPDF data over different data ranges we can extract information about the magnetic correlations on different length scales. The average magnetic order parameter (AMOP) is the long-range ordered moment. This reflects typical order parameter behavior, but dies above T_C as illustrated in Fig. 3.4. The local magnetic order parameter (LMOP) is the correlated magnetic moment between the nearest neighbor spins. As seen in Fig. 3.4, the LMOP shows quite different behavior from the AMOP; instead of vanishing at T_C, it survives well into the paramagnetic phase. The persistence of the LMOP well above T_C is direct evidence that short-range magnetic correlations remain in MnSb to very high temperatures, consistent with the previously mentioned idea that short-range magnetic correlations above T_C are responsible for the structural response observed above T_C from the structural PDF data.

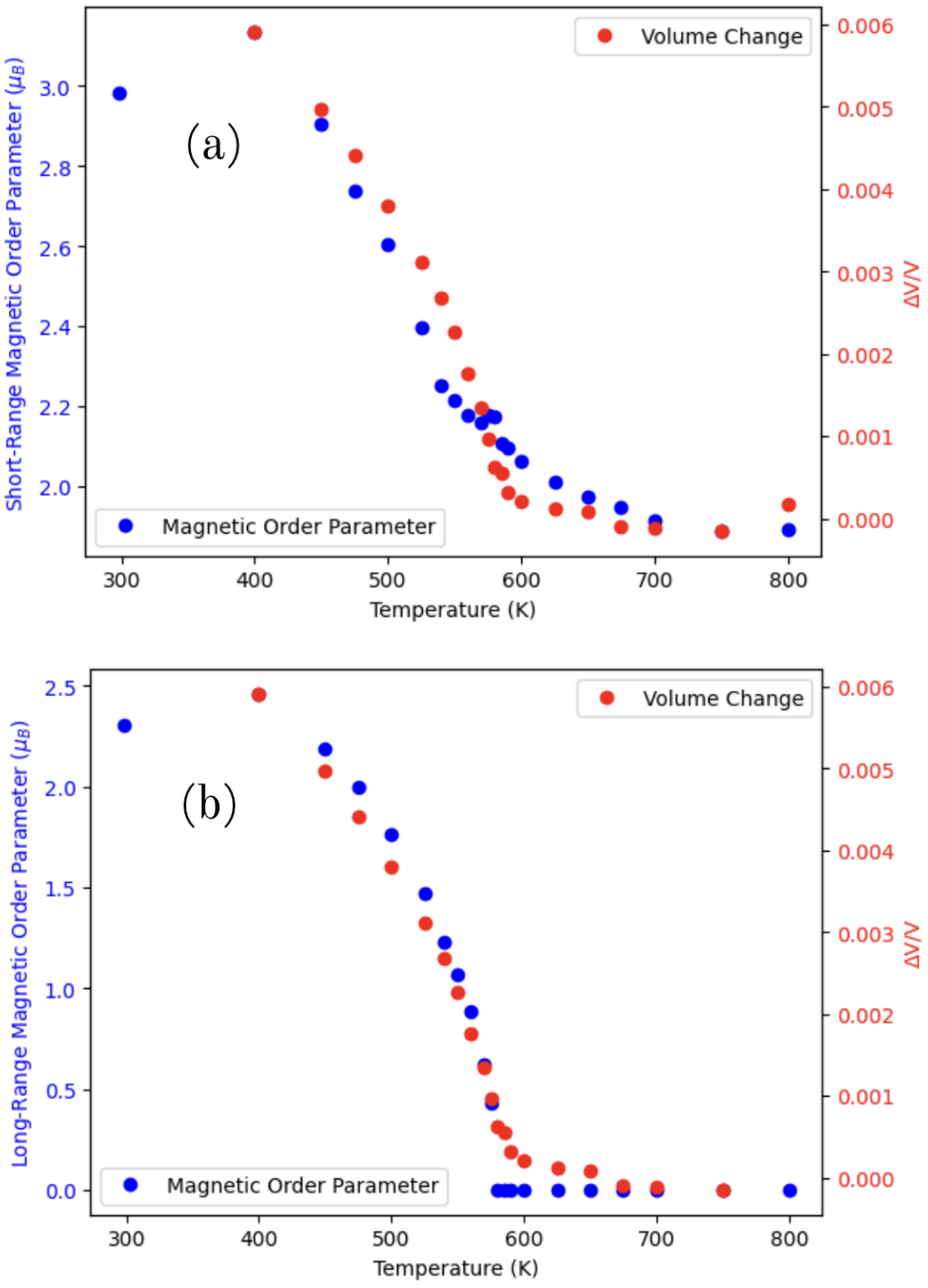

Figure 3.5 ΔV/V and Magnetic order Parameters as functions of temperature. Note that the volume change begins above T_C tracking roughly with the short-range magnetic correlations above T_C

4 Discussion

The experimental results revealed a large spontaneous magnetostriction effect in MnSb that begins well above the $577K$ Curie temperature, causing an expansion of the unit cell volume relative to the high-temperature linear thermal expansion trend. In addition, the neutron PDF data demonstrated that robust short-range magnetic correlations survive well above T_C. The forced magnetostriction appears to be somewhat small in magnitude compared to the spontaneous effect, and there was a clear but unexpected temperature dependence. There are robust short-range magnetic correlations that survive well above T_C. The forced magnetostriction appears to be somewhat small in magnitude compared to the spontaneous effect, and there was a clear but unexpected temperature dependence.

Our findings build upon previous studies of MnSb. The data confirm strong magnetostructural coupling, and provide greater detail regarding the temperature dependence and spatial anisotropy of the lattice response to the magnetic order. The observed temperature dependence of the forced magnetostriction response introduces a new dimension to this coupling. It suggests a more complex interplay between thermal energy and magnetic ordering than previously documented. While earlier studies have explored lattice distortions in response to magnetic fields, fewer have investigated temperature-dependent variations, making our results an important contribution to this area [6]. Additionally, the anisotropic response of the a and c lattice parameters across the Curie temperature deviates from expectations based on conventional magnetostructural transitions, where lattice distortions are often assumed to be more isotropic. The magnitude of spontaneous magnetostriction

was also notably large. This suggests a need to revisit existing models of structural response in MnSb and similar materials. Comparison with neutron scattering data further reinforces these findings, offering independent verification and highlighting the complementary nature of x-ray and neutron-based techniques.

The lattice response to the applied magnetic field is unique at different set temperatures. This suggests a complex interplay between thermal energy and magnetic ordering. This could be due to either a change in the magnetization process at different temperatures, thermal expansion effects, which might interfere with or enhance magnetostriction, or a shift in the balance between competing magnetic interactions as temperature increases.

The differing behavior of the a and c lattice parameters across the Curie temperature reflects the anisotropy of bonding and magnetic interactions in MnSb. Bonds within the basal plane differ fundamentally from those connecting adjacent planes, leading to distinct elastic and magnetic exchange strengths along the a and c directions. This directional dependence results in unequal lattice responses during the magnetic phase transition near 577 K. The asymmetry is evident in both the x-ray and neutron scattering data, confirming that it arises from intrinsic structural and magnetic properties rather than experimental uncertainty. Anisotropic lattice responses have also been observed in MnTe [2]. However, in the case of MnTe, the c lattice had a larger response than the a.

The most intriguing finding from our research is the deviation of the lattice parameters from their high-temperature linear trend beginning above 600K and well above T_C of 577 K. This is around the same temperature where the short-range magnetic correlations start grow in magnitude and correlation length. As seen in Fig. 4.1 there is roughly linear coupling between the unit cell volume and the LMOP above T_C. The coupling between the volume and the AMOP crosses over and becomes roughly quadratic below T_C. Conventionally, we would expect purely quadratic coupling at temperatures below T_C, and purely linear coupling above the transition temperature. This is the

behavior we observed in antiferromagnetic MnTe, which shares the same crystal structure type as MnSb [2]. This unique behavior from MnSb motivates further theoretical investigations into the mechanisms of magnetostructural coupling in MnSb and related materials.

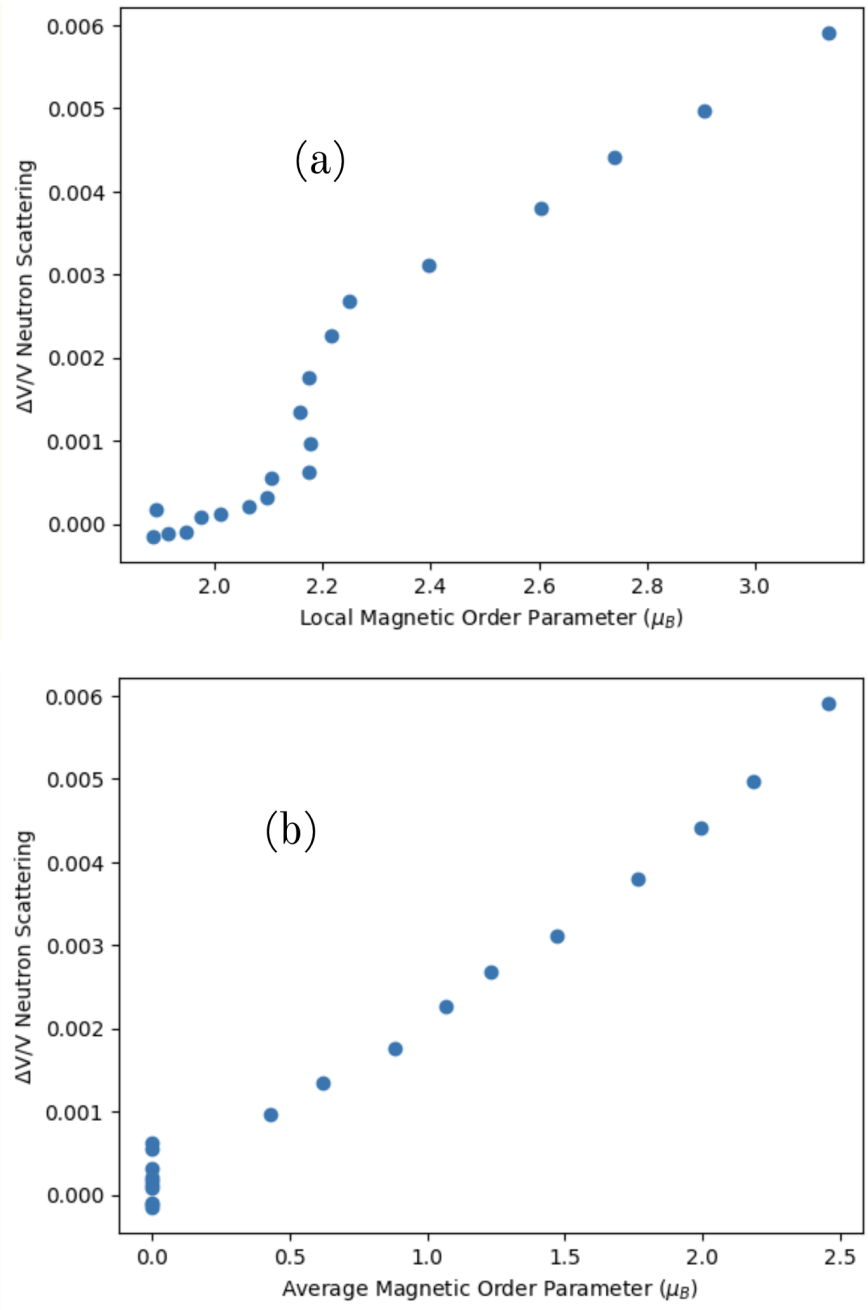

Figure 4.1 Magnetic order parameters as functions of ΔV/V. The conventional theory is that the relationship between the fractional volume change and the AMOP will be quadratic and there should be no coupling in the paramagnetic phase. What we see in the data is linear relationship between LMOP and the fractional volume change in the paramagnetic phase, and quadratic relationship with AMOP in ferromagnetic phase.

5 Conclusion

In summary, our findings confirm strong magnetostructural coupling in MnSb, as evidenced by changes in the lattice parameters in response to an external magnetic field. This behavior, relevant to magnetocaloric and magnetostrictive applications, invites comparison with other magnetostructural materials. Additionally, the observed temperature-dependent magnetostriction suggests a complex interplay between thermal energy and magnetic ordering, raising questions about reversibility and persistence across a broader temperature range. The anisotropic response of the a and c lattice parameters across the Curie temperature reflects the directional dependence of interatomic bonding and magnetic exchange interactions, highlighting fundamental differences between in-plane and out-of-plane atomic environments. Future work should explore these anomalies through theoretical modeling and extended experimental analysis to better understand the fundamental mechanisms driving the behavior of MnSb.

Future studies should extend the temperature range of measurements to determine whether the observed magnetostriction behavior persists at lower or higher temperatures, particularly near quantum regimes or extreme thermal conditions. Future studies will deepen our understanding of magnetostructural coupling in MnSb by combining theoretical and experimental approaches. Theoretical investigations should address how short-range magnetic correlations drive long-range lattice responses. Experimentally, more sensitive forced magnetostriction measurements—particularly those extending to higher applied magnetic fields—could provide a clearer picture of the coupling

between magnetic and structural degrees of freedom. In addition, conducting similar studies on MnSb samples with excess interstitial Mn would be valuable, as this off-stoichiometry significantly lowers the Curie temperature and may impact the nature of the coupling [1]. Finally, comparative analysis with other promising magnetocaloric materials could help identify shared features or unique mechanisms, offering broader insight into design principles for efficient solid-state refrigerants.

A Python Code

```
import numpy as np
from scipy import integrate
from scipy.optimize import curve_fit, least_squares
from scipy.integrate import quad
import matplotlib.pyplot as plt



def plot_csv(file_name, x_col, y_col):
  df = pd.read_csv(file_name)
  array = df.values
  temp = file_name[:-9]
  x = np.array(array[:,0])
  y = np.array(array[:,1])
  coefficients = np.polyfit(x, y, 1)
  slope, intercept = coefficients

  # Generate and display the line of best fit
  line_of_best_fit = np.polyval(coefficients, x)
```

```
  plt.plot(x, line_of_best_fit, color='red', label='Line of Best Fit'
     )
  equation = f'y = {slope:.6f}x + {intercept:.2f}'
  plt.annotate(equation, xy=(0.5, 0.95), xycoords='axes fraction', ha
     ='center', fontsize=10, color='red')

  plt.plot(x[:-1],y[:-1],marker='o')
  plt.plot(x[-1],y[-1], marker='o')
  plt.xlabel(x_col)
  plt.ylabel(y_col)
  plt.savefig(file_name[:-4]+'.png', dpi=300, bbox_inches='tight')
  plt.show()
  return slope

m1 = plot_csv('10K_MnSb.csv','Magnet Field (Tesla)','a Lattice
   Parameter (Angstroms)');
m2 = plot_csv('100K_MnSb.csv','Magnet Field (Tesla)','a Lattice
   Parameter (Angstroms)');
m3 = plot_csv('150K_MnSb.csv','Magnet Field (Tesla)','a Lattice
   Parameter (Angstroms)');
m4 = plot_csv('200K_MnSb.csv','Magnet Field (Tesla)','a Lattice
   Parameter (Angstroms)');
m5 = plot_csv('250K_MnSb.csv','Magnet Field (Tesla)','a Lattice
   Parameter (Angstroms)');
m6 = plot_csv('300K_MnSb.csv','Magnet Field (Tesla)','a Lattice
   Parameter (Angstroms)');
```

```
m7 = plot_csv('350K_MnSb.csv','Magnet Field (Tesla)','a Lattice
   Parameter (Angstroms)');
m8 = plot_csv('400K_MnSb.csv','Magnet Field (Tesla)','a Lattice
   Parameter (Angstroms)');
m9 = plot_csv('450K_MnSb.csv','Magnet Field (Tesla)','a Lattice
   Parameter (Angstroms)');
m10 = plot_csv('500K_MnSb.csv','Magnet Field (Tesla)','a Lattice
   Parameter (Angstroms)');


n1 = plot_csv('10K_MnSb_c.csv','Magnet Field (Tesla)','c Lattice
   Parameter (Angstroms)');
n2 = plot_csv('100K_MnSb_c.csv','Magnet Field (Tesla)','c Lattice
   Parameter (Angstroms)');
n3 = plot_csv('150K_MnSb_c.csv','Magnet Field (Tesla)','c Lattice
   Parameter (Angstroms)');
n4 = plot_csv('200K_MnSb_c.csv','Magnet Field (Tesla)','c Lattice
   Parameter (Angstroms)');
n5 = plot_csv('250K_MnSb_c.csv','Magnet Field (Tesla)','c Lattice
   Parameter (Angstroms)');
n6 = plot_csv('300K_MnSb_c.csv','Magnet Field (Tesla)','c Lattice
   Parameter (Angstroms)');
n7 = plot_csv('350K_MnSb_c.csv','Magnet Field (Tesla)','c Lattice
   Parameter (Angstroms)');
n8 = plot_csv('400K_MnSb_c.csv','Magnet Field (Tesla)','c Lattice
   Parameter (Angstroms)');
n9 = plot_csv('450K_MnSb_c.csv','Magnet Field (Tesla)','c Lattice
   Parameter (Angstroms)');
```

```
n10 = plot_csv('500K_MnSb_c.csv','Magnet Field (Tesla)','c Lattice
   Parameter (Angstroms)');

slopes_a= [n1,n2,n3,n4,n5,n6,n7,n8,n10]
slopes_c= [m1,m2,m3,m4,m5,m6,m7,m8,m10]
y_values_a = slopes_a/(np.sum(slopes_a)/len(slopes_a))
y_values_c = slopes_c/(np.sum(slopes_c)/len(slopes_c))
temps = [10,100,150,200,250,300,350,400,500]

fig, ax = plt.subplots()

# Plot the first graph (y = x)
ax.plot(temps, y_values_a, label="a lattice slope", color="blue",
   marker='o')

# Plot the second graph (y = x^2)
ax.plot(temps, y_values_c, label="c lattice slope", color="red",
   marker='o')

# Add a legend
ax.legend()

# Add labels and title
ax.set_xlabel("Temperature (K)")
ax.set_ylabel("Lattice (Angstroms)")
ax.set_title("Change in Lattice vs Temperature")
plt.grid(True)
```

```
# Show the plot
plt.show()
plt.savefig("Slopes.png")


data1=np.genfromtxt('c-vs-T-cooling.dat', skip_header=6)  # import
   lattice a
data2=np.genfromtxt('a-vs-T-cooling.dat',skip_header=6) # import
   lattice c


# Load the data, skipping the header
data3 = np.loadtxt('a_1p5-20.txt', skiprows=1)
data4 = np.loadtxt('c_1p5-20.txt', skiprows=1)
data5 = np.loadtxt('mvals_long-range_30-45.txt', skiprows=1)
data6 = np.loadtxt('mvals_short-range_1p5-20.txt', skiprows=1)


# Extract the columns. Note "_n" indicates neutron data and "m"
   indicates magnetic data other data is from atomic xray data
T_n = data3[:, 0]  # Temperature (first column)
a_n = data3[:, 1]  # a parameter (third column)
c_n = data4[:, 1]  # c parameter (third column)
T_m = data5[:, 0]  # Temperature (first column)
m_long = data5[:, 1]  # magnetic order parameter (third column)
m_short= data6[:, 1]  # magnetic order parameter (third column)


T = data1[:,0]+273.15 #temperature data in kelvin
a = data2[:,1] #a lattice parameter
c = data1[:,1] #c lattice parameter
```

```
v = np.sqrt(3)/2*a**2*c #volume


def func(p, T): # for fixed TD and variable alpha
    alpha, v0 = p
    fn = lambda x: x**3/(np.exp(x)-1)
    debye_int = np.array ([integrate.quad(fn,0,TD/t)[0]for t in T])
    debye_equ = alpha*1e30 * (9 * 4 * 1.38e-23)*T*(T/TD)**3*debye_int
        # alpha=gamma/B0
    #debye_equ = alpha*T**4/TD**3*debye_int
    #debye_equ = alpha*745200000*T**4/TD**3*debye_int
    return debye_equ + v0

def resid(p, T, data):
    return func(p, T) - data

def func2(p, T): # for fixed alpha and variable TD
    TD, v0 = p
    alpha = 1.68302497e-02
    fn = lambda x: x**3/(np.exp(x)-1)
    debye_int = np.array ([integrate.quad(fn,0,TD/t)[0]for t in T])
    debye_equ = alpha*T*(T/TD)**3*debye_int # alpha=gamma/B0
    #debye_equ = alpha*T**4/TD**3*debye_int
    #debye_equ = alpha*745200000*T**4/TD**3*debye_int
    return debye_equ + v0

def resid2(p, T, data):
    return func2(p, T) - data
```

```
def funcsingle_linear(p, T): # for single lattice parameter
    alpha, a0 = p
    fn = lambda x: x**3/(np.exp(x)-1)
    debye_int = np.array ([integrate.quad(fn,0,TD/t)[0]for t in T])
    debye_equ = alpha*1e30 * (9 * 4 * 1.38e-23)*T*(T/TD)**3*debye_int
        # alpha=gamma/B0
    #debye_equ = alpha*T**4/TD**3*debye_int
    #debye_equ = alpha*745200000*T**4/TD**3*debye_int
    return (debye_equ + a0**3)

def funcsingle(p, T): # for single lattice parameter
    alpha, a0 = p
    fn = lambda x: x**3/(np.exp(x)-1)
    debye_int = np.array ([integrate.quad(fn,0,TD/t)[0]for t in T])
    debye_equ = alpha*1e30 * (9 * 4 * 1.38e-23)*T*(T/TD)**3*debye_int
        # alpha=gamma/B0
    #print(debye_equ)
    #debye_equ = alpha*T**4/TD**3*debye_int
    #debye_equ = alpha*745200000*T**4/TD**3*debye_int
    return np.abs((debye_equ + a0**3))**0.3333

def residsingle(p, T, data):
    return funcsingle(p, T) - data

length=len(T)
step = (T[-1]-T[0])/length-0.35    # Step size
```

```
Tnew = np.linspace(T[0], T[0] + step * (length - 1), length)
mask = Tnew>650


mask=T>700
fig=plt.figure()

def line(params, x):
  m, b = params
  return m * x + b

def residuals(params, T, v):
    y = line(params, T)
    return v - y



##Volume data vs linear fit and fractional difference plots


# Initial guess for slope and intercept
x0 = [6.75825271e-03, 4.02]


# Perform least squares fitting
opt = least_squares(residuals, x0, args=(T[mask], v[mask]))
coefs = opt.x
vxline = line(opt.x, T)
print(opt.x)
plt.plot(T, v, 'o')
plt.xlabel('T (K)')
```

```
plt.ylabel('v ($A^{3}$)')
plt.title('volume vs temp with linear fit MnSb')
plt.plot(T, vxline)
plt.show()

#Plot fractional difference between line and data
FDiffvx=(v-vxline)/v
plt.figure()
plt.plot(T,FDiffvx)
plt.title('fractional difference between data and fit')
plt.show()

## a lattice parameter data vs linear fit and fractional difference
   plots
fig=plt.figure()
mask = T>740

def line(params, x):
  m, b = params
  return m * x + b

def residuals(params, T, a):
    y = line(params, T)
    return a - y

# Initial guess for slope and intercept
x0 = [1.3e-11, 4.02]
```

```
# Perform least squares fitting
opt = least_squares(residuals, x0, args=(T[mask], a[mask]))
coefs= opt.x
axline = line(opt.x, T)
plt.plot(T, a, 'o')
plt.xlabel('T (K)')
plt.ylabel('a (A)')
plt.title('a lattice with linear fit MnSb')
plt.plot(T, axline)
plt.show()

#Plot fractional difference between line and data
FDiffax=(a-axline)/a
plt.figure()
plt.plot(T,FDiffax)
plt.title('fractional difference between data and fit')
plt.show()

## c lattice parameter data vs linear fit and fractional difference
   plots
plt.figure()
mask = T>650

def line(params, x):
  m, b = params
  return m * x + b
```

```
def residuals(params, T, c):
    y = line(params, T)
    return c - y

# Initial guess for slope and intercept
x0 = [1.3e-11, 4.02]

# Perform least squares fitting
opt = least_squares(residuals, x0, args=(T[mask], c[mask]))
coefs = opt.x
cxline = line(opt.x, T)
plt.plot(T, c, 'o')
plt.xlabel('T (K)')
plt.ylabel('c (  )')
plt.title('c lattice with linear fit MnSb')
plt.plot(T, cxline)
plt.show()

#Plot fractional difference between line and data
plt.figure()
FDiffcx=(c-cxline)/c
plt.figure()
plt.plot(T,FDiffcx)
plt.title('fractional difference between data and fit')
plt.show()
```

```
plt.figure()
mask = T>650


def line(params, x):
  m, b = params
  return m * x + b


def residuals(params, T, c):
    y = line(params, T)
    return c - y


# Initial guess for slope and intercept
x0 = [1.3e-11, 4.02]


# Perform least squares fitting
opt = least_squares(residuals, x0, args=(T[mask], c[mask]))
coefs = opt.x
cxline = line(opt.x, T)
plt.plot(T, c, 'o')
plt.xlabel('T (K)')
plt.ylabel('c (A)')
plt.title('c lattice with linear fit MnSb')
plt.plot(T, cxline)
plt.show()


#Plot fractional difference between line and data
plt.figure()
```

```
FDiffcx=(c-cxline)/c
plt.figure()
plt.plot(T,FDiffcx)
plt.title('fractional difference between data and fit')
plt.show()

## Neutron Volume data vs linear fit and fractional difference graphs

v_n=np.sqrt(3)/2*a_n**2*c_n
fig=plt.figure()
mask = T_n>620



def line(params, x):
  m, b = params
  return m * x + b

def residuals(params, T, a):
    y = line(params, T)
    return a - y

# Initial guess for slope and intercept
x0 = [1.3e-11, 4.02]

# Perform least squares fitting
opt = least_squares(residuals, x0, args=(T_n[mask], v_n[mask]))
coefs= opt.x
```

```
print(opt.x)
slope_n=opt.x[0]


vnline = line(opt.x, T_n)
plt.plot(T_n, v_n, 'o')
plt.xlabel('T_n (K)')
plt.ylabel('volume ($A^{3}$)')
plt.title('volume with linear fit MnSb')
plt.plot(T_n, vnline)
plt.show()


#Plot fractional difference between line and data
plt.figure()
FDiffvn=(v_n-vnline)/v_n
plt.figure()
plt.scatter(T_n,FDiffvn)
plt.title('fractional difference between data and fit')
plt.show()


## Comparing Neutron and X-ray Data


plt.figure()
plt.plot(T_n[1:], v_n[1:],'o', label='Neutron')
plt.plot(Tnew, v,'o', label='X-ray')
plt.plot(T_n, vnline, label='xray fit')
plt.plot(Tnew, vxline, label= 'neutron fit')
```

```
plt.xlabel('T (K)')
plt.ylabel('volume ($A^{3}$)')
plt.legend()


plt.figure()
plt.scatter(T_n[1:],FDiffvn[1:],label='Neutron')
plt.scatter(Tnew,FDiffvx,label='X-ray')
plt.xlabel('T (K)')
plt.ylabel('fractional volume difference')
plt.legend()
plt.show()


plt.figure()


##LMOP and dV/V vs Temperature
# Create primary y-axis
fig, ax1 = plt.subplots()


# Plot magnetic parameter on the primary y-axis
ax1.plot(T_m, m_short, 'bo', label='Magnetic Order Parameter')
ax1.set_xlabel("Temperature (K)")
ax1.set_ylabel(r'Short-Range Magnetic Order Parameter ($\mu_B$)',
   color='b')
ax1.tick_params(axis='y', labelcolor='b')


# Create secondary y-axis
ax2 = ax1.twinx()
```

```
ax2.plot(T_n[1:], FDiffvn[1:], 'ro', label='Volume Change')
ax2.set_ylabel("dV/V", color='r')
ax2.tick_params(axis='y', labelcolor='r')

# Legends
ax1.legend(loc="lower left")
ax2.legend(loc="upper right")

#plt.title("LMOP and dV/V vs Temperature")
plt.show()

plt.figure()

# Create primary y-axis
fig, ax1 = plt.subplots()

##AMOP and dV/V vs Temperature
# Plot magnetic parameter on the primary y-axis
ax1.plot(T_m, m_long, 'bo', label='Magnetic Order Parameter')
ax1.set_xlabel("Temperature (K)")
ax1.set_ylabel(r'Long-Range Magnetic Order Parameter ($\mu_B$)',
   color='b')
ax1.tick_params(axis='y', labelcolor='b')

# Create secondary y-axis
ax2 = ax1.twinx()
ax2.plot(T_n[1:-1], FDiffvn[1:-1], 'ro', label='Volume Change')
```

```
ax2.set_ylabel("dV/V", color='r')
ax2.tick_params(axis='y', labelcolor='r')


# Legends
ax1.legend(loc="lower left")
ax2.legend(loc="upper right")


#plt.title("AMOP and dV/V vs Temperature")
plt.show()


##Neutron LMOP and AMOP vs fractional difference


plt.scatter(m_short[1:], FDiffvn[1:])
plt.xlabel(r'Local Magnetic Order Parameter ($\mu_B$)')
plt.ylabel("dV/V Neutron Scattering")
#plt.title("LMOP vs. dV/V")
plt.show()


plt.scatter(m_long[1:], FDiffvn[1:])
plt.xlabel(r'Average Magnetic Order Parameter ($\mu_B$)')
plt.ylabel("dV/V Neutron Scattering")
#plt.title("AMOP vs. dV/V")
plt.show()
```

Bibliography

[1] J. A. Cooley, M. K. Horton, E. E. Levin, S. H. Lapidus, K. A. Persson, and R. Seshadri, "From Waste-Heat Recovery to Refrigeration: Compositional Tuning of Magnetocaloric $Mn_{1+x}Sb$," Chemistry of Materials **32,** 1243–1249 (2020).

[2] R. Baral, A. M. Abeykoon, B. J. Campbell, and B. A. Frandsen, "Giant Spontaneous Magnetostriction in MnTe Driven by a Novel Magnetostructural Coupling Mechanism," Advanced Functional Materials **33,** 2305247 (2023).

[3] T. Chatterji, B. Ouladdiaf, and D. Bhattacharya, "Neutron diffraction investigation of the magnetic structure and magnetoelastic effects in $NdMnO_3$," Journal of Physics: Condensed Matter **21,** 306001 (2009).

[4] "BNL | National Synchrotron Light Source II,".

[5] Y. Onodera, T. Sato, and S. Kohara, "X-Ray and Neutron Pair Distribution Function Analysis," in *Hyperordered Structures in Materials: Disorder in Order and Order within Disorder*, K. Hayashi, ed., (Springer Nature, Singapore, 2024), pp. 93–120.

[6] P. B. D. Castro *et al.*, "Machine-learning-guided discovery of the gigantic magnetocaloric effect in HoB2 near the hydrogen liquefaction temperature," NPG Asia Materials **12,** 35 (2020).

Index